

ELECTRICALLY SILENT MAGNETIC FIELDS

BRADLEY J. ROTH AND JOHN P. WIKSWO, JR.

Department of Physics and Astronomy, Vanderbilt University, Nashville, Tennessee 37235

ABSTRACT There has been a significant controversy over the past decade regarding the relative information content of bioelectric and biomagnetic signals. In this paper we present a new, theoretical example of an electrically-silent magnetic field, based on a bidomain model of a cylindrical strand of tissue generalized to include off-diagonal components in the conductivity tensors. The physical interpretation of the off-diagonal components is explained, and analytic expressions for the electrical potential and the magnetic field are found. These expressions show that information not obtainable from electrical potential measurements can be obtained from measurements of the magnetic field in systems with conductivity tensors more complicated than those previously examined.

INTRODUCTION

Speculation that electrically silent magnetic fields may be produced by electrically active tissue began with the very first biomagnetic measurements (1), and a controversy over their existence has continued to this day (2-9). In 1982, Plonsey presented one of the more mathematical analyses, suggesting that measurement of the external bioelectric field completely determines the external biomagnetic field (5). In this paper, we present a theoretical example of a biomagnetic field that cannot be determined from the bioelectric field. We term such a magnetic field as "electrically silent" because information about the tissue is present in the magnetic signal while absent in the electric signal. Our example is based on an electrically active strand of tissue that has a "spiral-like" or "helix-like" conductivity, represented by off-diagonal terms in the conductivity tensor. Such a conductivity tensor can arise in multicellular tissues that have a complicated cellular geometry. We shall first review the standard calculation of the potential and magnetic field of an electrically active fiber, and then show how this calculation can be generalized to describe strands of more complex multicellular tissues that can give rise to electrically silent magnetic fields.

MATHEMATICAL DERIVATION OF THE MODEL

A Scalar Conductivity

The electrical potential, Φ , and the magnetic field, \mathbf{B} , produced by a cylindrical fiber, such as a single unmyeli-

nated nerve axon, can be calculated from the transmembrane potential, Φ_m , using a volume conductor model (10, 11). We assume that an action potential propagates along the fiber in the axial, z , direction with velocity u , and that the fiber, of radius a , lies in an unbounded external bath with conductivity σ_e . We further assume that all the fields are quasistationary, and are measured at a radial distance ρ from the center of the fiber. The electrical properties of the intracellular cytoplasm can be described by a scalar conductivity, σ_i , so that the current density inside the fiber, \mathbf{J}_i , is given by Ohm's law

$$\mathbf{J}_i = \sigma_i \mathbf{E}_i, \quad (1)$$

with the intracellular electric field, \mathbf{E}_i , given in terms of the intracellular potential, Φ_i , as

$$\mathbf{E}_i = -\nabla \Phi_i. \quad (2)$$

The fundamental equation governing the quasistatic distribution of current in a volume conductor is the continuity equation,

$$\nabla \cdot \mathbf{J} = 0. \quad (3)$$

Combining the continuity equation with Ohm's law and the relationship between the potential and the electric field, we find that the intracellular potential is governed by Laplace's equation

$$\nabla^2 \Phi_i = 0. \quad (4)$$

The potential in the bath, Φ_e , is also governed by Laplace's equation, and Φ_i and Φ_e are coupled by the boundary conditions at the fiber surface (10, 11). Since there is no preferred angle, θ , the problem is cylindrically symmetric,

Address reprint requests to John P. Wiksw, Jr., Department of Physics and Astronomy, Vanderbilt University, Box 1807 Station B, Nashville, TN 37235

so that Eq. 4 reduces to

$$\frac{1}{\rho} \frac{\partial}{\partial \rho} \left(\rho \frac{\partial \Phi_i}{\partial \rho} \right) + \frac{\partial^2 \Phi_i}{\partial z^2} = 0. \quad (5)$$

This equation can be solved analytically for the potential and current density inside the fiber (10). Since the potential is independent of θ and the azimuthal component of the current density, J_θ^i , is proportional to $\partial \Phi_i / \partial \theta$, there is no component of the current density in the azimuthal direction. The remaining two components of the current density produce a magnetic field that is entirely azimuthal (11). This magnetic field has a one-to-one correspondence to the electrical potential, so that no information is present in one signal while absent in the other¹. In this case, there are no electrically silent magnetic fields.

A Diagonal Tensor Conductivity

A multicellular strand of tissue, such as a cardiac Purkinje fiber, is more complicated than a single nerve axon because of the underlying cellular geometry and interstitial space. Ganapathy et al. (12) have modeled a strand of syncytial tissue as a single "equivalent cell" with different intracellular conductivities in the axial and radial directions. This model accounts for the anisotropy of the tissue, but not for the interstitial space. A better way to represent such a strand is to use a bidomain model (13–17)². Both the intracellular (*i*) and interstitial (*o*) conductivities have been represented as diagonal tensors, so that Ohm's law in each medium becomes

$$\begin{pmatrix} J_i^r \\ J_i^\theta \\ J_i^z \end{pmatrix} = \begin{pmatrix} \sigma_i^r & 0 & 0 \\ 0 & \sigma_i^\theta & 0 \\ 0 & 0 & \sigma_i^z \end{pmatrix} \begin{pmatrix} E_i^r \\ E_i^\theta \\ E_i^z \end{pmatrix}, \quad (6)$$

$$\begin{pmatrix} J_o^r \\ J_o^\theta \\ J_o^z \end{pmatrix} = \begin{pmatrix} \sigma_o^r & 0 & 0 \\ 0 & \sigma_o^\theta & 0 \\ 0 & 0 & \sigma_o^z \end{pmatrix} \begin{pmatrix} E_o^r \\ E_o^\theta \\ E_o^z \end{pmatrix}. \quad (7)$$

The conductivity may be different in the $\hat{\rho}$, $\hat{\theta}$ and \hat{z} directions, and may be different in the intracellular and interstitial media. In such a bidomain model, the components of the conductivity tensors must be considered as homogeneous, macroscopic parameters, useful when calculating the electric potential or current density averaged over many cells, but not applicable on the cellular level, where the tissue may be quite inhomogeneous.

¹ The transmembrane resting potential is an exception to the one-to-one correspondence between the electric potential and magnetic field. We could say that the resting potential is produced by a "magnetically silent electric field".

² A more extensive bibliography of papers using bidomain models is given in reference (17).

In a syncytium, the equation of continuity becomes (13, 14)

$$\nabla \cdot (J_i + J_o) = 0. \quad (8)$$

Using this equation and Eqs. 6 and 7, and assuming cylindrical symmetry, we find that the potentials in the intracellular medium, Φ_i , and the interstitial medium, Φ_o , satisfy the equation (17)

$$\frac{1}{\rho} \frac{\partial}{\partial \rho} \left[\rho \frac{\partial}{\partial \rho} (\sigma_i^r \Phi_i + \sigma_o^r \Phi_o) \right] + \frac{\partial^2}{\partial z^2} (\sigma_i^z \Phi_i + \sigma_o^z \Phi_o) = 0. \quad (9)$$

By assuming that the transmembrane potential is independent of ρ (restricting our attention to action potentials that propagate uniformly along the z -axis), we can use Eq. 9 to derive analytical expressions for the potential and current density in the intracellular and interstitial media, and from the current density we can calculate the magnetic field (17). We find that there is no azimuthal component of the current density in either medium, the magnetic field is in the $\hat{\theta}$ direction, and there is a one-to-one correspondence between the magnetic field and the electrical potential (17). Again, no electrically silent magnetic fields arise.

A Full Tensor Conductivity

The diagonal conductivity tensors in Eqs. 6 and 7 constrain the direction of most or least resistance to current flow to be either axial, radial or azimuthal³. This is adequate for a Purkinje fiber, in which the cells all lie parallel to the axis of the tissue strand. But what if the cells have a more complicated geometry, perhaps being twisted around each other like the individual fibers in a braided rope? This would require a more general conductivity tensor containing off-diagonal terms. In this case, Ohm's law for the intracellular and interstitial media becomes

$$\begin{pmatrix} J_i^r \\ J_i^\theta \\ J_i^z \end{pmatrix} = \begin{pmatrix} \sigma_i^{rr} & \sigma_i^{r\theta} & \sigma_i^{rz} \\ \sigma_i^{\theta r} & \sigma_i^{\theta\theta} & \sigma_i^{\theta z} \\ \sigma_i^{zr} & \sigma_i^{z\theta} & \sigma_i^{zz} \end{pmatrix} \begin{pmatrix} E_i^r \\ E_i^\theta \\ E_i^z \end{pmatrix}, \quad (10)$$

$$\begin{pmatrix} J_o^r \\ J_o^\theta \\ J_o^z \end{pmatrix} = \begin{pmatrix} \sigma_o^{rr} & \sigma_o^{r\theta} & \sigma_o^{rz} \\ \sigma_o^{\theta r} & \sigma_o^{\theta\theta} & \sigma_o^{\theta z} \\ \sigma_o^{zr} & \sigma_o^{z\theta} & \sigma_o^{zz} \end{pmatrix} \begin{pmatrix} E_o^r \\ E_o^\theta \\ E_o^z \end{pmatrix}. \quad (11)$$

The presence of off-diagonal components in the conductivity tensor is neither mysterious nor unprecedented. The diagonal tensors in Eqs. 6 and 7 would have off-diagonal terms if expressed in other coordinate systems, such as spherical. Full tensor conductivities are commonly used when describing the electrical properties of an anisotropic

³ The "directions of most and least resistance" is a nonmathematical way of referring to the eigenvectors of the conductivity tensor.

crystal (18). Off-diagonal components of the conductivity tensor were applied to a biological system by Mathias (19) when studying a skeletal muscle fiber with a "helicoidal" transverse-tubule system. He states that "the tilt of the T system plane might cause a component of the radial current to be projected onto the longitudinal axis; radial voltage gradients in the T system would then drive part of the longitudinal current in the fiber. The longitudinal continuity of the T system could set up a cablelike network within the fiber, so that longitudinal voltage gradients in the sarcoplasm might drive current in the T system." Such a conductivity could also arise in a multicellular tissue when the underlying cellular geometry is complicated.

The conductivity tensor is always symmetric (18), and therefore has three independent off-diagonal terms, each of which has a physical interpretation. If $\sigma_i^{\theta\rho}$ is nonzero, then the preferred current path (the direction of highest conductivity) in the intracellular medium in a plane perpendicular to the z -axis is not in the radial or azimuthal directions, but at some angle between them. Current following the path of least resistance traces out a spiral, as in Fig. 1 *a*. We will say that a conductivity tensor with a nonvanishing $\sigma_i^{\theta\rho}$ has a "spiral-like" conductivity. If $\sigma_i^{\theta z}$ is nonzero, then the path of least resistance in a cylindrical shell of constant radius ρ does not lie parallel to \hat{z} or $\hat{\theta}$. In this case, the intracellular current tends to follow a helical path, as in Fig. 1 *b*. We will say that a medium with a nonvanishing $\sigma_i^{\theta z}$ has a "helix-like" conductivity. If $\sigma_i^{\rho z}$ is nonzero, then the direction of highest conductivity in a plane of constant θ does not lie parallel to the ρ or z axes, so that the intracellular current spreads out as if flowing over a cone, as in Fig. 1 *c*. We will say that a medium with a nonvanishing $\sigma_i^{\rho z}$ has a "cone-like" conductivity. Similar interpretations can be made for the interstitial medium.

Cylindrical symmetry is not broken by the introduction

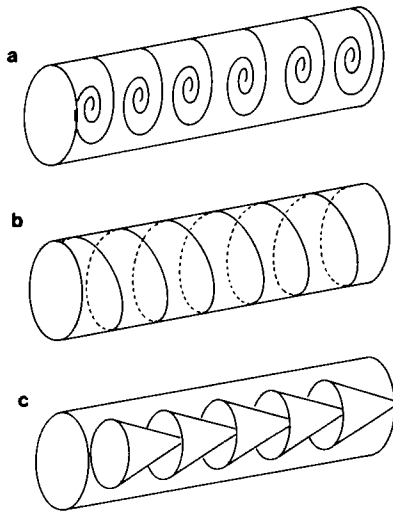


FIGURE 1 The path of least resistance in a tissue with (a) a spiral-like conductivity, $\sigma_i^{\theta\rho} \neq 0$, (b) a helix-like conductivity, $\sigma_i^{\theta z} \neq 0$, and (c) a cone-like conductivity, $\sigma_i^{\rho z} \neq 0$.

of off-diagonal terms into the conductivity tensor; there is still no preferred angle so that all fields are independent of θ . Using this fact, Eqs. 10 and 11, and the continuity equation, we find that the potentials in the intracellular and interstitial media are governed by the equation

$$\begin{aligned} \frac{1}{\rho} \frac{\partial}{\partial \rho} \left[\rho \frac{\partial}{\partial \rho} (\sigma_i^{\rho\rho} \Phi_i + \sigma_o^{\rho\rho} \Phi_o) \right] + \frac{\partial^2}{\partial z^2} (\sigma_i^{zz} \Phi_i + \sigma_o^{zz} \Phi_o) \\ + \frac{1}{\rho} \frac{\partial}{\partial \rho} \left[\rho \frac{\partial}{\partial z} (\sigma_i^{\rho z} \Phi_i + \sigma_o^{\rho z} \Phi_o) \right] \\ + \frac{\partial^2}{\partial z \partial \rho} (\sigma_i^{\theta z} \Phi_i + \sigma_o^{\theta z} \Phi_o) = 0. \quad (12) \end{aligned}$$

The off-diagonal components $\sigma_i^{\rho z}$ and $\sigma_o^{\rho z}$ appear in Eq. 12, but $\sigma_i^{\theta\rho}$, $\sigma_i^{\theta z}$, $\sigma_o^{\theta\rho}$ and $\sigma_o^{\theta z}$ do not. For the remainder of our discussion, we consider the case in which $\sigma_i^{\rho z}$ and $\sigma_o^{\rho z}$ are equal to zero, i.e. the conductivity is not cone-like, so that Eq. 12 is identical to Eq. 9. The boundary conditions are unchanged by $\sigma_i^{\theta\rho}$, $\sigma_i^{\theta z}$, $\sigma_o^{\theta\rho}$, and $\sigma_o^{\theta z}$, so that the potential with these four off-diagonal components present will be exactly the same as the potential due to a diagonal conductivity tensor. As far as voltage measurements are concerned, the two situations are indistinguishable, even in the immediate vicinity of the active region of tissue. The only electrical measurements that might be capable of detecting the off-diagonal terms would be ones that detect the potential distribution at the cellular-level, where the concept of homogeneous, macroscopic intracellular and interstitial conductivities is not applicable. Analytical expressions for the electric potentials inside and outside the strand are summarized in the Appendix. The parameters $\sigma_i^{\theta\rho}$, $\sigma_i^{\theta z}$, $\sigma_o^{\theta\rho}$, and $\sigma_o^{\theta z}$ are not present in these expressions.

The current density inside the strand will not be the same, however. The components of the intracellular current density can be written as

$$J_i^{\rho} = -\sigma_i^{\rho\rho} \frac{\partial \Phi_i}{\partial \rho}, \quad (13)$$

$$J_i^{\theta} = -\sigma_i^{\theta\rho} \frac{\partial \Phi_i}{\partial \rho} - \sigma_i^{\theta z} \frac{\partial \Phi_i}{\partial z}, \quad (14)$$

$$J_i^z = -\sigma_i^{zz} \frac{\partial \Phi_i}{\partial z}. \quad (15)$$

Similar equations exist for the interstitial current density. The component of the intracellular current density in the $\hat{\theta}$ direction depends on $\sigma_i^{\theta\rho}$ and $\sigma_i^{\theta z}$, and will not vanish, even though we maintain cylindrical symmetry. It is this component of the current density that ultimately leads to electrically silent magnetic fields.

The Magnetic Field

The magnetic field can be calculated from the current density using the law of Biot and Savart

$$\mathbf{B} = \frac{\mu_0}{4\pi} \int \frac{\mathbf{J} \times (\mathbf{r} - \mathbf{r}')}{|\mathbf{r} - \mathbf{r}'|^3} dV, \quad (16)$$

which can be rewritten as

$$\mathbf{B} = \frac{\mu_0}{4\pi} \left\{ \int \frac{\nabla \times \mathbf{J}}{|\mathbf{r} - \mathbf{r}'|} dV + \int \frac{\mathbf{J} \times \mathbf{n}}{|\mathbf{r} - \mathbf{r}'|} dS \right\}. \quad (17)$$

For the cylindrically symmetric case, the source terms in the integrands in Eq. 17 can be written as

$$\nabla \times \mathbf{J} = -\frac{\partial J^\theta}{\partial z} \rho + \left(\frac{\partial J^\rho}{\partial z} - \frac{\partial J^z}{\partial \rho} \right) \theta + \frac{1}{\rho} \frac{\partial}{\partial \rho} (\rho J^\theta) \mathbf{z} \quad (18)$$

and

$$\mathbf{J} \times \mathbf{n} = -J^\theta \mathbf{z} + J^z \theta. \quad (19)$$

If either $\sigma_i^{\theta\rho}$, $\sigma_i^{\theta z}$, $\sigma_i^{\rho\theta}$, or $\sigma_i^{\rho z}$ is not zero, then J^θ does not vanish and there exists components of the magnetic field in the ρ and z directions. We can consider these two components as the "electrically silent" components of the magnetic field. Analytic expressions for the magnetic field, based on Eqs. 17 through 19, are derived in the Appendix. The absence of $\sigma_i^{\theta\rho}$, $\sigma_i^{\theta z}$, $\sigma_i^{\rho\theta}$, and $\sigma_i^{\rho z}$ from the expression for the electrical potential but their presence in the expression for the magnetic field is the key point of this paper. It is the reason we claim that the magnetic field contains information not present in the electric potential.

In this example we not only can show the existence of electrically silent magnetic fields but also can determine their size and spatial dependence. Fig. 2 is a schematic representation of the current density and the magnetic field corresponding to a strand of tissue with a spiral-like conductivity. The azimuthal component of the current density, which produces the axial and radial components of the magnetic field, is closely related to the radial component of the current density. Using the expressions in the Appendix, we can calculate the magnetic field from the

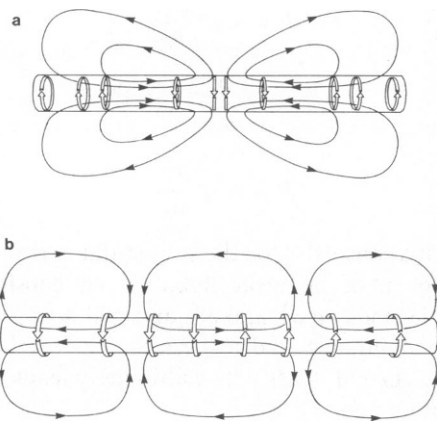


FIGURE 2 A schematic drawing of the (a) current density and (b) magnetic field produced by an action potential propagating down a strand of tissue with a spiral-like conductivity. In a, the current density at any point in the strand is the vector sum of the axial and radial components (solid lines) and the azimuthal component (bands). A similar scheme was used to represent the components of the magnetic field in b. The figure is a qualitative drawing, not meant to be quantitatively correct.

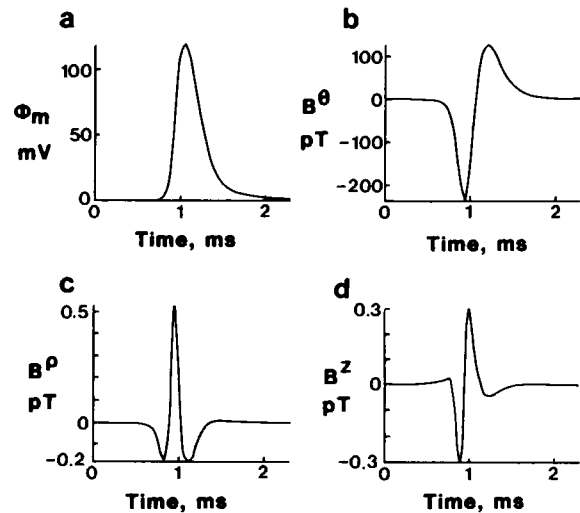


FIGURE 3 (a) The transmembrane potential, $\Phi_m(z)$, used as the basis for the calculation. The calculated magnetic field: (b) the azimuthal component, B^θ , (c) the radial component B^ρ , and (d) the axial component, B^z . The parameters used in this calculation are $a = 0.1$ mm, $\rho = 1$ mm, $u = 15$ m \cdot s $^{-1}$, and all the components of the conductivity tensors, as well as the bath conductivity, are equal to $1 \Omega^{-1}\text{m}^{-1}$.

transmembrane potential, as shown in Fig. 3. The parameters used in this calculation are $a = 0.1$ mm, $\rho = 1$ mm, $u = 15$ m \cdot s $^{-1}$, and all nonzero components of the conductivity tensors, as well as the conductivity of the bath, are set equal to $1 \Omega^{-1}\text{m}^{-1}$. Qualitatively, the azimuthal component of the magnetic field, B^θ , is proportional to the first derivative of the transmembrane potential, the radial component, B^ρ , is proportional to the third derivative, and the axial component, B^z , is proportional to the fourth derivative. The amplitudes of B^ρ and B^z are small relative to B^θ , but can be increased by making a larger. For $a = 1$ mm, the radial and axial components of the magnetic field have peak-to-peak amplitudes $\sim 10\%$ as large as the azimuthal component.

There exists a nonzero azimuthal component B^θ of the magnetic field in all cases we have discussed, but the azimuthal component of the current density is nonzero only for spiral-like or helix-like conductivities. This component does not vanish because the laws of magnetostatics follow a "right-hand rule" that determines the direction of the field. The laws of electrostatics have no such "handedness," so if the tissue geometry does not provide this handedness, then there is nothing to distinguish between a positive or negative J^θ (clockwise or counterclockwise around the z -axis), and J^θ must be zero. A conductivity tensor with a nonvanishing $\sigma_i^{\theta\rho}$ or $\sigma_i^{\theta z}$ gives a handedness to the tissue, breaking the symmetry just enough to allow an azimuthal component of the current density.

DISCUSSION

It is useful to compare the electrically silent magnetic field calculated in this paper to those suggested by others. The usual procedure for discussing the independence of the

magnetic and electric fields is to write expressions for the magnetic field and the electric potential in terms of the curl and divergence of an "impressed" current density, \mathbf{J}_i , that is the biological source of the volume conducted current (2, 20). Wikswo and Barach (6) postulate a divergenceless component of \mathbf{J}_i that is electrically silent but magnetically detectable. The point of view of this paper is somewhat different, since our electrically silent magnetic fields are produced by Ohmic, volume-conducted currents instead of non-Ohmic impressed currents. However, both models require a similar spiraling or helical tissue geometry to produce azimuthal, or toroidal, current loops. The equivalent impressed current density discussed by Wikswo and Barach (6) is in fact the macroscopic result of a true membrane current impressed upon a conductor with off-diagonal terms in the conductivity tensor.

The impressed current density can also be investigated by taking a multipole expansion of \mathbf{J}_i (7, 9). Wikswo (7) shows that the antisymmetric part of the current quadrupole tensor can produce electrically silent magnetic fields. Since any antisymmetric tensor has vanishing diagonal components, it is clear that only the off-diagonal components of the current quadrupole tensor lead to electrically silent magnetic fields. An analogy to our calculation is again evident, since in both calculations it is the off-diagonal terms of a tensor that generate electrically silent magnetic fields; in our case, the conductivity tensor, and in Wikswo's case, the current quadrupole tensor. Our present analysis provides a local mechanism for producing current patterns described by an antisymmetric quadrupole tensor that were previously thought to exist on only a much larger scale.

The model in this paper was derived specifically for strands of cardiac or smooth muscle syncytia with unusual cellular geometries. It is not clear if such strands occur in nature, but they might be created in the laboratory by either growing strands in cell cultures or by carefully twisting ordinary muscle bundles. However, the model may apply to other tissues which do occur naturally. For instance, it might be used to model single isolated skeletal muscle fibers, for which the interstitial medium represents the transverse-tubular system. There is evidence that the T-tubules in skeletal muscle are "helicooids" (21), which implies that the interstitial conductivity will contain off-diagonal terms. If the myofibrils are helical (21), the intracellular conductivity might also contain off-diagonal terms. The implications of this T system geometry on the electrical properties of a muscle fiber has been studied by Mathias (19). He concluded that an effect would exist, but that it would be small because the tubules were tilted at a very small angle relative to the transverse plane of the fiber.

Electrically silent magnetic fields are not restricted to syncytial tissues. The conductivity of the passive, nonsyncytial tissue surrounding an active fiber in a nerve bundle or skeletal muscle is an important parameter in calculating

the compound action potential or electromyogram. If these passive tissues have unusual cellular geometries, their conductivities might contain off-diagonal terms, leading to electrically silent magnetic fields. The myelin sheath surrounding a nerve axon is one such example of a spiraling tissue geometry.

Syncytial and nonsyncytial tissues that do not have the cylindrical geometry discussed in this paper may also produce electrically silent magnetic fields if the underlying cellular geometry is complicated enough. The apex of the heart is an obvious example of a tissue with a spiraling cellular geometry (B. J. Roth, W.-Q. Guo, and J. P. Wikswo, Jr., manuscript in preparation). In fact, the geometry of cardiac muscle is complicated enough (22) that we feel it would be surprising if electrically silent magnetic fields are not produced by the electrical activity of the heart. This may have ramifications for experimental comparisons of the electrocardiogram and the magnetocardiogram, and for the interpretation of the types of current pathways that are responsible for re-entry-associated arrhythmogenesis.

CONCLUSION

If we accept the existence of off-diagonal terms in the conductivity tensor, then this paper proves that the magnetic field can contain information that is absent in the electric potential. The obvious question is whether such electrically silent magnetic fields occur in nature? We have presented several tissues which have a cellular or sub-cellular geometry with a spiraling or helical structure. Our calculations suggest that electrically silent magnetic fields may be produced in these tissues, implying that it may be possible to obtain new information about these biological tissues from their magnetic field. Whether this possibility can be exploited experimentally remains to be seen.

APPENDIX

The geometry of a cylindrical strand of tissue is simple enough that the electric potential and the magnetic field can be calculated analytically. We shall restrict our attention to the case of a strand, of radius a , having a "spiral-like" conductivity, so that σ_{rz}^z , $\sigma_{\theta\theta}^z$, $\sigma_{\theta z}^z$, and $\sigma_{z\theta}^z$ vanish, but $\sigma_{\theta\theta}^z$ and $\sigma_{\theta z}^z$ do not. If we express the transmembrane potential $\Phi_m(z)$ in terms of its Fourier transform, $\phi_m(k)$, where

$$\Phi_m(z) = \frac{1}{2\pi} \int_{-\infty}^{\infty} \phi_m(k) e^{-ikz} dk, \quad (A1)$$

and

$$\phi_m(k) = \int_{-\infty}^{\infty} \Phi_m(z) e^{+ikz} dz, \quad (A2)$$

then we find that the Fourier transforms of the intracellular potential, $\phi_i(\rho, k)$, the interstitial potential, $\phi_o(\rho, k)$, and the external potential, $\phi_e(\rho, k)$, are (17)

$$\phi_i(\rho, k) = \frac{\sigma_i^{zz}}{\sigma_i^{zz} + \sigma_o^{zz}} \left[\frac{I_0(|k|\lambda\rho)}{I_0(|k|\lambda a)\beta(|k|, a, \lambda)} + \frac{\sigma_o^{zz}}{\sigma_i^{zz}} \right] \phi_m(k), \quad (A3)$$

$$\phi_o(\rho, k) = \frac{\sigma_i^{zz}}{\sigma_i^{zz} + \sigma_o^{zz}} \left[\frac{I_0(|k|\lambda\rho)}{I_0(|k|\lambda a)\beta(|k|, a, \lambda)} - 1 \right] \phi_m(k), \quad (A4)$$

and

$$\phi_e(\rho, k) = \frac{K_0(|k|\rho)}{K_0(|k|a)\alpha(|k|, a, \lambda)} \phi_m(k), \quad (\text{A5})$$

with

$$\alpha(|k|, a, \lambda) = -\left[\left(\frac{\sigma_i^{zz} + \sigma_o^{zz}}{\sigma_i^{zz}}\right) + \gamma(|k|, a, \lambda)\right], \quad (\text{A6})$$

$$\beta(|k|, a, \lambda) = 1 + \left(\frac{\sigma_i^{zz} + \sigma_o^{zz}}{\sigma_i^{zz}}\right) \frac{1}{\gamma(|k|, a, \lambda)}, \quad (\text{A7})$$

$$\gamma(|k|, a, \lambda) = \lambda \frac{\sigma_e K_1(|k|a) I_0(|k|\lambda a)}{\sigma_i^{zz} I_1(|k|\lambda a) K_0(|k|a)}, \quad (\text{A8})$$

and

$$\lambda = \sqrt{\frac{\sigma_i^{zz} + \sigma_o^{zz}}{\sigma_i^{\theta\theta} + \sigma_o^{\theta\theta}}}. \quad (\text{A9})$$

The parameters $\sigma_i^{\theta\theta}$ and $\sigma_o^{\theta\theta}$ do not appear in the above equations. The potential is not changed by the presence of a "spiral-like" conductivity.

The Fourier transform of the magnetic field outside the strand ($\rho > a$), is given by

$$B^{\theta}(\rho, k) = \mu_0 a I_1(|k|a) K_1(|k|\rho) i k \times \left[\frac{\sigma_i^{zz}}{\beta(|k|, a, \lambda)} \delta(|k|, a, \lambda) - \frac{\sigma_e}{\alpha(|k|, a, \lambda)} \right] \phi_m(k), \quad (\text{A10})$$

$$B^e(\rho, k) = -\mu_0 a I_1(|k|a) K_1(|k|\rho) i k \frac{(\sigma_i^{\theta\theta} + \sigma_o^{\theta\theta})}{\beta(|k|, a, \lambda)} \times \frac{\lambda^2}{\lambda^2 - 1} [1 - \delta(|k|, a, \lambda)] \phi_m(k), \quad (\text{A11})$$

$$B^z(\rho, k) = \mu_0 a I_0(|k|a) K_0(|k|\rho) |k| \frac{(\sigma_i^{\theta\theta} + \sigma_o^{\theta\theta})}{\beta(|k|, a, \lambda)} \lambda \frac{I_1(|k|\lambda a)}{I_0(|k|\lambda a)} \times \left[1 + \frac{\lambda^2}{1 - \lambda^2} \left(1 - \frac{1}{\lambda^2 \delta(|k|, a, \lambda)} \right) \right] \phi_m(k), \quad (\text{A12})$$

where

$$\delta(|k|, a, \lambda) = \frac{I_1(|k|\lambda a) I_0(|k|a)}{\lambda I_0(|k|\lambda a) I_1(|k|a)}. \quad (\text{A13})$$

In the limit when $\sigma_i^{\theta\theta} + \sigma_o^{\theta\theta} = \sigma_i^{zz} + \sigma_o^{zz} (\lambda - 1)$, Eqs. A10 through A12 reduce to

$$B^{\theta}(\rho, k) = \mu_0 a I_1(|k|a) K_1(|k|\rho) i k \times \left[\frac{\sigma_i^{zz}}{\beta(|k|, a, \lambda)} - \frac{\sigma_e}{\alpha(|k|, a, \lambda)} \right] \phi_m(k), \quad (\text{A14})$$

$$B^e(\rho, k) = -\mu_0 a I_1(|k|a) K_1(|k|\rho) i k |k| a (\sigma_i^{\theta\theta} + \sigma_o^{\theta\theta}) \times \frac{I_1(|k|a)}{2 I_0(|k|a) \beta(|k|, a, \lambda)} \times \left[1 + \frac{2 I_0(|k|a)}{|k| a I_1(|k|a)} - \left(\frac{I_0(|k|a)}{I_1(|k|a)} \right)^2 \right] \phi_m(k), \quad (\text{A15})$$

$$B^z(\rho, k) = \mu a I_0(|k|a) K_0(|k|\rho) |k| (\sigma_i^{\theta\theta} + \sigma_o^{\theta\theta}) \frac{I_1(|k|a)}{\beta(|k|, a, \lambda) I_0(|k|a)} \times \left[1 - \frac{|k|a}{2} \left(\frac{I_0(|k|a)}{I_1(|k|a)} - \frac{I_1(|k|a)}{I_0(|k|a)} \right) \right] \phi_m(k). \quad (\text{A16})$$

The radial and axial components of the magnetic field are both proportional to $(\sigma_i^{\theta\theta} + \sigma_o^{\theta\theta})$.

We thank John Barach and the reviewers for their helpful comments.

This work was supported in part by the office of Naval Research under Contract N00014-82-K-0107, and National Institute of Health Grant 1-R01 NS 19794.

REFERENCES

1. Baule, G. M., and R. Mcfee. 1963. Detection of the magnetic field of the heart. *Am. Heart J.* 66:95-96.
2. Plonsey, R. 1972. Capability and limitations of electrocardiography and magnetocardiography. *IEEE (Inst. Electr. Electron. Eng.) Trans. Biomed. Eng.* BME-19:239-244.
3. Rush, S. 1975. On the independence of magnetic and electric body surface recordings. *IEEE (Inst. Electr. Electron. Eng.) Trans. Biomed. Eng.* BME-22:157-167.
4. Cohen, D. 1975. Magnetic fields of the human body. *Physics Today*. 28:34-43.
5. Plonsey, R. 1982. The nature of sources of bioelectric and biomagnetic fields. *Biophys. J.* 39:309-312.
6. Wikswo, J. P., Jr., and J. P. Barach. 1982. Possible sources of new information in the magnetocardiogram. *J. Theor. Biol.* 95:721-729.
7. Wikswo, J. P., Jr. 1983. Theoretical aspects of the ECG-MCG relationship. In *Biomagnetism, An Interdisciplinary Approach*. S. Williamson, G. Romani, L. Kaufman, and I. Modena, editors. Plenum Publishing Corp., NY. 311-326.
8. Titomir, L. I., and P. Kneppo. 1983. On the possibility to determine integral characteristics of the cardiac electric generator from extracardiac electric and magnetic measurements. *IEEE (Inst. Electr. Electron. Eng.) Trans. Biomed. Eng.* BME-30:222-226.
9. Titomir, L. I., and P. Kneppo. 1985. Simultaneous analysis of the cardiac electric and magnetic fields using the scalar multipole expansion. *Bull. Math. Biol.* 47:123-143.
10. Clark, J. W., Jr., and R. Plonsey. 1968. The extracellular potential field of the single nerve axon in a volume conductor. *Biophys. J.* 8:842-864.
11. Woosley, J. K., B. J. Roth, and J. P. Wikswo, Jr. 1985. The magnetic field of a single axon: A volume conductor model. *Math. Biosci.* 76:1-36.
12. Ganapathy, N., J. W. Clark, Jr., O. B. Wilson, and W. Giles. 1985. Forward and inverse potential field solutions for cardiac strands of cylindrical geometry. *IEEE (Inst. Electr. Electron. Eng.) Trans. Biomed. Eng.* BME-32:566-577.
13. Tung, L. 1978. A bidomain model for describing ischemic myocardial dc potentials. Ph. D. dissertation, Massachusetts Inst. Technol., Cambridge.
14. Geselowitz, D. B., and W. T. Miller, III. 1983. A bidomain model for anisotropic cardiac muscle. *Ann. Biomed. Eng.* 11:191-206.
15. Plonsey, R., and R. C. Barr. 1982. The four-electrode resistivity technique as applied to cardiac muscle. *IEEE (Inst. Electr. Electron. Eng.) Trans. Biomed. Eng.* BME-29:541-546.
16. Yamashita, Y., and D. B. Geselowitz. 1985. Source-field relationships for cardiac generators on the heart surface based on their transfer coefficients. *IEEE (Inst. Electr. Electron. Eng.) Trans. Biomed. Eng.* BME-32:964-970.

17. Roth, B. J., and J. P. Wikswo, Jr. 1986. A bidomain model for the extracellular potential and magnetic field of cardiac tissue. *IEEE (Inst. Electr. Electron. Eng.) Trans. Biomed. Eng.* BME-33:467-469.
18. Landau, L., and E. Lifshitz. 1960. *Electrodynamics of Continuous Media*. Pergamon Press, New York, NY.
19. Mathias, R. T. 1978. An analysis of the electrical properties of a skeletal muscle fiber containing a helicoidal T system. *Biophys. J.* 23:277-284.
20. Geselowitz, D. B. 1970. On the magnetic field generated outside an inhomogeneous volume conductor by internal current sources. *IEEE (Inst. Electr. Electron. Eng.) Trans. Mag.* Mag-6:346-347.
21. Peachey, L. D., and B. R. Eisenberg. 1978. Helicoids in the T system and striations of frog skeletal muscle fibers seen by high voltage electron microscopy. *Biophys. J.* 22:145-154.
22. Streeter, D. 1979. Gross Morphology and Fiber Geometry of the Heart. *In Handbook of Physiology, Sec. 2: The Cardiovascular System*. Ed. Stephen R. Geiger.